PHILOSOPHICAL TRANSACTIONS OF THE ROYAL SOCIETY A
MATHEMATICAL, PHYSICAL & ENGINEERING SCIENCES

Solar and stellar flares

T. G. Forbes

Phil. Trans. R. Soc. Lond. A 2000 **358**, 711-727
doi: 10.1098/rsta.2000.0554

THE ROYAL SOCIETY

Solar and stellar flares

By T. G. Forbes

EOS Institute, The University of New Hampshire, Durham, NH 03824, USA

New observations by space telescopes during the last ten years have led to significant advances in understanding the nature of solar flares. X-ray and UV imaging of flare emissions have confirmed that flares are powered by the sudden release of magnetic energy associated with currents flowing in the solar atmosphere. Although many different processes have been suggested as possible trigger mechanisms, the one which seems to fit the observations best is a loss of ideal-MHD equilibrium, or stability, combined with magnetic reconnection. An ideal-MHD process by itself has the drawback that it releases a very small amount of magnetic energy, but when it is coupled with magnetic reconnection, this drawback is eliminated. Stellar flares are very likely to be fundamentally similar to solar flares in that they involve the sudden release of magnetic energy associated with currents flowing in their coronae. However, it is unlikely that they all involve exactly the same type of field configuration or the same type of trigger mechanism. What these mechanisms might be will be difficult to determine without further information on the structure of stellar magnetic fields.

Keywords: solar flares; stellar flares; magnetohydrodynamics; magnetic fields; reconnection; flare models

1. Introduction

In the solar atmosphere there are three different types of large-scale eruptive phenomena which are all thought to be manifestations of a single physical process. These phenomena are *flares*, *coronal mass ejections* (CMEs) and *prominence eruptions*. What they have in common is that they all involve a disruption of the coronal magnetic field.

If the disruption occurs in an active region (i.e. a region with sunspots), then it creates the bright patches of emission on the surface which traditionally define a flare. (The emissions, called *flare ribbons*, are best seen in Hα, and they occur in the chromosphere, the layer lying just above the photosphere.) If the disruption occurs outside an active region, the surface emissions may be too weak to be considered a standard flare, and usually such disruptions go unnoticed, unless they lead to an ejection of mass into interplanetary space, known as a CME. Large flares almost always produce a CME, but small flares rarely do so.

More than half of all CMEs are associated with the eruption of large *quiescent prominences*. These prominences are dense clouds of cool partly ionized plasma which are supported against gravity by a coronal magnetic field which is locally horizontal in the vicinity of the prominence. In order for a horizontal field to exist, strong currents must flow within the corona itself, and it is the disruption of these currents which leads to the eruption of a prominence. CMEs not associated with a prominence eruption probably occur in regions where the coronal current does not have sufficient strength or the right orientation to support a prominence.

For reasons discussed in § 5, stellar flares are thought to involve the same fundamental process as that occurring in solar flares, namely the release of magnetic energy stored in a star's atmosphere. However, as more data are obtained about flare stars, it seems increasingly likely that the field configurations involved may be quite different. This is almost a foregone conclusion for binary systems where interaction between the fields of both stars are involved, and it is also likely to be true for the classic dMe and dKe flare stars. (The names refer to their spectral type.) These are rapidly rotating red dwarfs which may have rotation periods as small as 10 h and whose magnetic field structure may, therefore, be more like Jupiter's than the Sun's.

One can speculate that the difference in the flare process from one star to another is as varied as the process which creates auroral magnetic substorms in the different planetary magnetospheres of our solar system. In the case of Jupiter, such substorms are caused by the disruption of the current sheet created by Jupiter's rapid 10 h rotation (Zimbardo 1993), but in the case of the Earth, they are caused by the disruption of the *geomagnetic-tail* current sheet created by the drag of the solar wind on the terrestrial magnetic field (Hones 1973). In both cases the fundamental process is the release of stored magnetic energy, but the differences in the field structures involved make it impossible for a single theoretical model to describe them both.

2. Magnetic energy storage

One of the most important aspects of solar and stellar flares is that they occur in a plasma environment dominated by magnetic fields. In the solar atmosphere, magnetic energy is the only source of energy that is capable of producing the radiative and kinetic energy output of large flares. Before the onset of a solar flare the magnetic energy density ($B^2/(2\mu_0)$, where μ_0 is the permeability of free space) of a 100 G (10^{-2} T) coronal field is *ca.* 40 J m^{-3}. By comparison, the thermal energy density (nkT, where k is Boltzman's constant) is *ca.* 0.01 J m^{-3}, since the coronal particle density, n, and temperature, T, are *ca.* 10^{15} m^{-3} and 10^6 K, respectively. Finally, the kinetic energy density ($\frac{1}{2}m_\mathrm{p}nv^2$, where m_p is the proton rest mass) in the corona is *ca.* 10^{-6} J m^{-3} assuming that the velocity, v, is of the order of 1 km s^{-1}—the convective velocity imparted by flows at the photospheric level. The gravitational energy density ($m_\mathrm{p}ngh$, where g is the solar surface gravity of 247 m s^{-2}) is of the order of 0.04 J m^{-3} assuming that the average mass height, h, is *ca.* 10^8 m. Thus, the magnetic energy density is about three orders of magnitude greater than any of the other types. Since large flares typically have an energy of 10^{25} J (10^{32} erg) and a volume in the range 10^{24}–10^{25} m^3, an average energy density of 1–10 J m^{-3} is required. Only the magnetic energy density is in this range, so non-magnetic models of flares are ruled out.

Sunspots and other magnetic features in the solar photosphere are unaffected by the occurrence of flares. This is because the plasma in the photosphere is almost 10^9 times denser than the plasma in the corona where flares originate, so it is very difficult for disturbances in the tenuous corona to affect the extremely massive plasma of the photospheric layer. Field lines mapping from the corona to the photosphere are said to be inertially line-tied to the photosphere, meaning that the footpoints of coronal field lines are effectively stationary over the time-scale of a flare.

The time-scale for the onset of solar flares is very rapid. From observations it has been estimated that as much as 10^{25} J (10^{32} erg) is generated in the form of thermal and kinetic energy during the first few minutes after onset. This is an extremely short time-scale for an organized process to be occurring over a region whose size is of the order of 10^5 km (about 10 times larger than the diameter of the Earth), and it implies dynamic velocities of the order of 100 to 1000 km s^{-1}—close to the speed at which magnetic and acoustic waves propagate in the corona. The implication of such a large energy output in so short a time is that *ca.* 10% of the available magnetic energy in a volume of 10^{15} km^3 is converted to thermal and kinetic energy within a few wave travel times. In other words, flares require an onset mechanism which processes magnetic energy with an efficiency of the order of 10% on a time-scale which is only a few times greater than the wave travel time. This combination of efficiency and speed is not easy to explain theoretically.

3. Trigger mechanism

At the present time, the most generally accepted explanation for the cause of flares is that they are produced by a loss of instability or equilibrium in the coronal magnetic field. The continual emergence of new flux from the convection zone and the shuffling of the footpoints of closed coronal field lines causes stresses to build up in the coronal field. Eventually, the stress exceeds a threshold beyond which a stable equilibrium cannot be maintained, and the field erupts. The eruption releases the magnetic energy stored in the stressed field, so models based on this mechanism are sometimes referred to as *storage models*.

If the flare produces a CME, magnetic field lines mapping from the ejected plasma to the photosphere are stretched outwards to form an extended open-field structure. This opening of the field creates an apparent paradox, since the stretching of the field lines implies that the magnetic energy of the system is increasing, whereas storage models require it to decrease (Sturrock *et al*. 1984). Barnes & Sturrock (1972) argued that this paradox does not occur, because the relaxation of the stressed field which exists prior to the eruption releases more magnetic energy than is consumed in stretching the field lines. In other words, the magnetic energy required to open the field should be less than the free magnetic energy stored in the corona. Following this line of thought, Kopp & Pneuman (1976) proposed a scenario for a three-stage model of an eruptive flare. Prior to the eruption, energy is stored in a force-free arcade or flux rope. (A force-free field is one with the current flowing in the direction of the magnetic field.) Eventually the field erupts outwards to form a fully opened magnetic-field configuration. Finally, the opened configuration reconnects to form a closed, nearly current-free, field. According to Barnes & Sturrock (1972) the evolution from the first stage to the second would be an ideal-MHD process occurring on the Alfvén time-scale, while the evolution from the second stage to the third would be a resistive-MHD process occurring on the slower reconnection time-scale. Thus the middle stage would constitute a metastable state at an intermediate magnetic energy level.

Aly (1984, 1991) and Sturrock (1991) have shown that the above scenario is energetically impossible. Using quite general arguments they prove that the fully opened field configuration must always have a higher magnetic energy than the corresponding force-free magnetic field as long as the field is simply connected. This result has caused consternation among some theorists because it seems to imply that eruptive flares are energetically impossible. However, as Aly and Sturrock have noted, there are several ways to avoid this predicament. First, the magnetic fields may not be simply connected but contain X points and O points; second, an ideal-MHD eruption can still extend field lines as long as it does not open them all the way to infinity; and finally, an ideal-MHD eruption is possible if it only opens a portion of the closed field lines (Wolfson & Low 1992; Low & Smith 1993).

One type of storage model that has received much attention tries to create an eruption by shearing the footpoints of an arcade of loops (Mikić *et al*. 1988; Martinell 1990; Steinolfson 1991; Inhester *et al*. 1992; Aly 1994; Kusano *et al*. 1995; Amari *et al*. 1996). In two-dimensional force-free configurations with translational symmetry, shearing causes the arcade to expand smoothly outwards towards a fully opened state without ever producing an eruption. It is not yet known whether this is true for all three-dimensional configurations.

Even if shearing an arcade does not produce an ideal loss of equilibrium or stability, it is still possible to create a rapid eruption by invoking a resistive instability. For example, shearing an arcade may lead to the formation of a current sheet which can undergo reconnection (Somov 1992). If the reconnection occurs rapidly, say at a rate which is of the order of a few Alfvén time-scales, then a rapid eruption occurs (Mikić & Linker 1994). In order for this mechanism to work, the reconnection rate must undergo a sudden transition. Prior to the eruption it must be slow compared with the time-scale of the photospheric motions, so that energy can be stored in the coronal currents. After the eruption it must be fast, so that energy can be released rapidly. Thus, a complete model of the eruption process must explain why the reconnection rate suddenly changes at the time of the eruption. There are several possible mechanisms which could do this. For example, if the current sheet is subject to the tearing-mode instability, then reconnection will not occur until the length of the current sheet becomes longer than about 2π times its width (Furth *et al*. 1963). Alternatively, as the current sheet builds up, its current density may exceed the threshold of a microinstability which creates an anomalous resistivity (Heyvaerts & Priest 1976). The anomalous resistivity subsequently triggers rapid reconnection and the ejection of a flux rope.

Sheared arcades can also be formed by the emergence of a flux rope from below the photosphere as long as the central axis of the rope lies on or below the photosphere. However, if the flux-rope axis lies above the photosphere, then the arcade will contain a flux rope whose field lines are anchored only at its ends.

Figure 1 shows a two-dimensional flux-rope model which loses equilibrium when the photospheric sources of the field approach one another (Forbes & Priest 1995). The configuration is obtained by solving the Grad–Shafranov equation

$$\nabla^2 A + \frac{1}{2}\frac{\mathrm{d}B_z^2}{\mathrm{d}A} = 0 \tag{3.1}$$

in the semi-infinite xy-plane with $y \geqslant 0$, where B_z is the field perpendicular to the xy-plane and $A(x, y)$ is the flux function defined by

$$(B_x, B_y, B_z) = \left[\frac{\partial A}{\partial y}, -\frac{\partial A}{\partial x}, B_z(A)\right]. \tag{3.2}$$

The surface at $y = 0$ corresponds to the photosphere. Equation (3.1) is used to construct an evolutionary sequence of force-free equilibria by assuming that changes

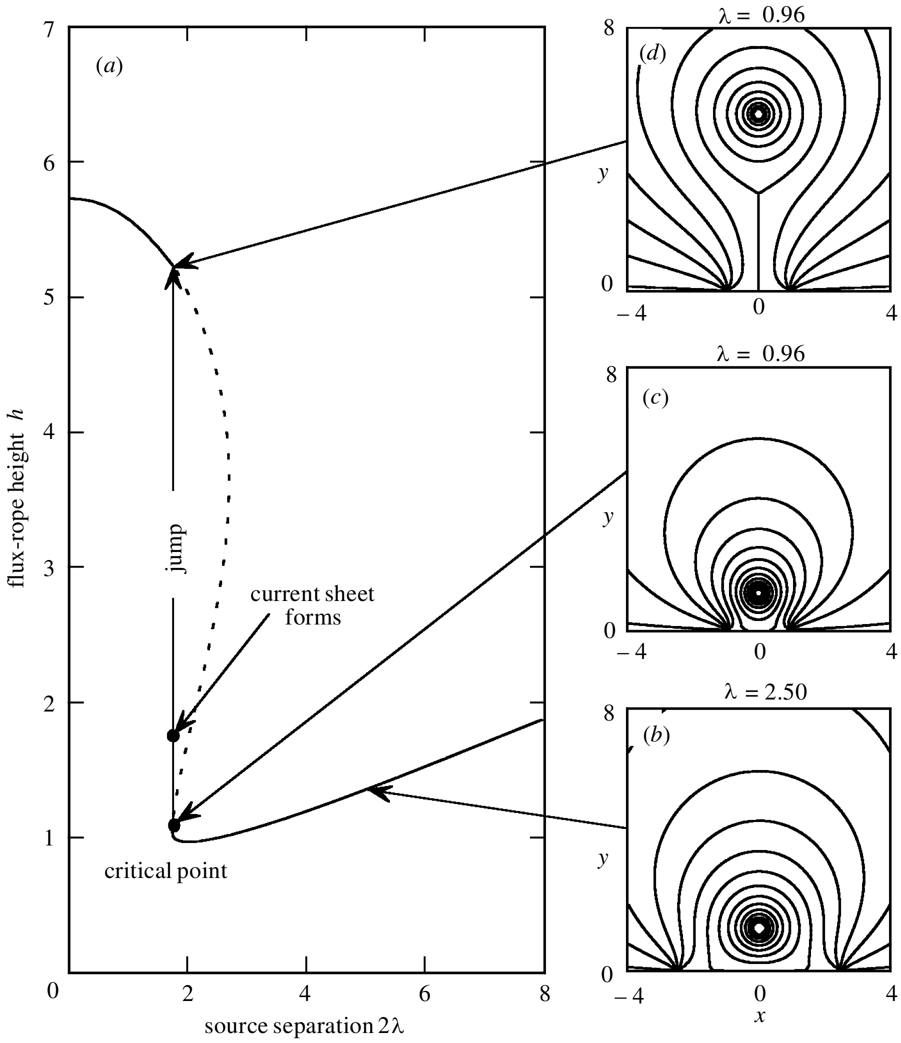

Figure 1. Ideal-MHD evolution of a two-dimensional arcade containing an unshielded flux rope. (*a*)–(*c*) The flux rope and arcade jumps upwards when the two photospheric field sources are pushed too close to one another. (*d*) In the absence of reconnection, the eruption leads to a new equilibrium containing a current sheet.

in the photospheric boundary conditions occur more slowly than the Alfvén timescale in the corona.

Figure 1*a* shows the equilibrium flux-rope height as a function of the source separation (2λ) for $a_0 = 0.1\lambda_0$. The S-shaped curve is characteristic of cusp-type catastrophes, where the highest and lowest branches are stable, but the middle branch is unstable (Poston & Stewart 1978). If one starts with a configuration corresponding to a point on the lower branch, as shown in figure 1*b*, and then move the source regions towards each other, a catastrophe will occur when λ reaches the point where the lower and middle branches of the equilibrium curve meet. At this point the configuration (figure 1*c*) loses magnetic equilibrium, and the flux rope is thrown upwards

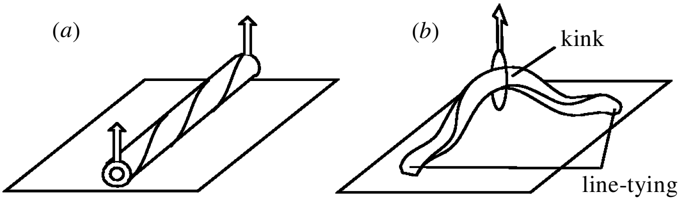

Figure 2. Comparison of (a) the two-dimensional flux-rope model with (b) a more realistic three-dimensional configuration. Several turns of the field are shown for illustrative purposes, but in reality, the number of turns is probably between one and two.

by the imbalance which develops between the magnetic compression and tension forces acting on it (Van Tend & Kuperus 1978; Yeh 1983; Martens & Kuin 1989; van Ballegooijen & Martens 1989).

What happens after the loss of equilibrium depends on the dynamics. If one assumes that there is no reconnection, and all the kinetic energy released by the loss of equilibrium is dissipated, then the flux rope restabilizes at the upper equilibrium shown in figure 1*d*. On the other hand, if this energy is not dissipated, then the flux rope oscillates up and down between the lower equilibrium at the catastrophe point and a height somewhere above the height of the upper equilibrium. Finally, if reconnection does occur, then the flux rope continues to move upwards indefinitely, although its upward motion may be slowed once its altitude exceeds the upper equilibrium height.

Because the model shown in figure 1 is two dimensional, it does not take into consideration what happens if the ends of the flux rope are anchored to the photosphere (i.e. line-tied), as is almost certain to be the case in reality. When the ends are anchored, as shown in figure 2, only the central portion of the flux rope has the possibility to move upwards. Consequently, the two-dimensional model corresponds to the onset of an *external kink* (as opposed to an *internal kink*, which leaves the outer surface of the flux rope unmoved). Hood (1990) has shown that the line-tying of the ends of a flux rope at a surface helps to stabilize it against kinking, but if the flux rope contains more than a couple of turns, line-tying alone can no longer stabilize it. Thus, an eruption can still occur, at least in principle, in a three-dimensional flux rope whose ends are anchored in the photosphere. Unfortunately, the two-dimensional model cannot be quantitatively applied to the three-dimensional case, because the kink instability is an inherently three-dimensional process.

4. Solar flare loops

The opening of the field lines in an active region by a large flare leads to the formation of flare ribbons and loops which can last for more than 10 h. These structures appear to move through the chromosphere and corona, and they provide some of the best evidence for reconnection in the solar atmosphere. Doppler-shift measurements show conclusively that the motions of the flare loops and ribbons are not due to mass motions of the solar plasma, but rather to the upward propagation of an energy source in the corona (see, for example, Schmieder *et al.* 1987). Such motions are exactly what one expects for a reconnection model of the flare loops.

Flare loops range from temperatures of 10^4 to 3×10^7 K, with the cooler loops nested below the hotter loops. They have traditionally been called 'post'-flare loops, but this is a misnomer since the energy release continues throughout their lifetime. Remarkably, the loops at the low temperature are two orders of magnitude cooler than the surrounding coronal plasma. These super-cool loops are formed from the hot loops by a radiative thermal instability (Cox 1972), which is possible in the solar atmosphere because of its non-black-body behaviour (Parker 1953).

The outermost edges of the hot X-ray loops map to the outer edge of the chromospheric flare ribbons (Schmieder *et al*. 1996), while the inner edges of the cool Hα loops map to the inner edge of the ribbons (Rust & Bar 1973). During the course of a flare, the separation between the ribbons increases, and the loops grow larger with time.

Magnetic reconnection (for a review see Priest & Forbes 1999) is thought by most researchers to be the only mechanism which can account for the motion of the flare loops and ribbons. Simple expansion of the loops due to outward motion of the plasma from the flare site has been ruled out by Doppler-shift measurements of the Hα loops. Doppler shifts in the Hα line show that the plasma in the cool loops flows downward at speeds of 100 to 500 km s^{-1} during the time that the loops appear to be expanding (see, for example, Schmieder *et al*. 1987). Thus, the loop motions are not due to mass motions of the plasma, but rather to the continual propagation of an energy source onto new field lines.

Although loop and ribbon motions are strong evidence for reconnection (Kopp & Pneuman 1976), the evidence they provide is circumstantial. In principle, X-ray telescopes of sufficient spatial resolution and sensitivity should be able to provide direct evidence by imaging the reconnection site itself as it moves upwards in the corona. However, the ability to determine whether or not there is a reconnection site in the corona depends very much on theoretical expectations of what such a site should look like. During the last few years, high-resolution images obtained from the X-ray telescopes on the Japanese satellite Yohkoh show several features that are highly suggestive of a reconnection site in the corona. These features include: a hard X-ray source located above the soft X-ray loops (Sakao *et al*. 1992; Masuda 1994; Bentley *et al*. 1994); cusp structures suggestive of either an X-type or a Y-type neutral line (Acton *et al*. 1992; Tsuneta 1993; Doschek *et al*. 1995); bright features at the top of the soft X-ray loops (Tsuneta *et al*. 1992; McTiernan *et al*. 1993); and high-temperature plasma along the field lines mapping to the tip of the cusp (Tsuneta 1996).

Some of the cusp-shaped loops observed by Yohkoh have a linear trunk-like feature which extends from the top of the cusp all the way down to the inner arch of the flare loop system. The hottest regions in the loop system do not lie in the trunk feature but along the edges of the cusp formed by the outermost loop (Tsuneta 1996), and the trunk feature is both cooler and denser than the plasma surrounding it.

Figure 3 shows a theoretical model which explains the loop structures in terms of the processes of reconnection and *chromospheric evaporation* (i.e. the ablation of the chromosphere by heat conduction and energetic particles). The figure incorporates the early ideas of Carmichael (1964), Sturrock (1968), Hirayama (1974), Kopp & Pneuman (1976) and Cargill & Priest (1982). However, most of the details of the figure come from the results of various simulations of reconnection (Forbes & Malherbe 1991), evaporation (Nagai 1980; Somov *et al*. 1982; Cheng 1983; Doschek *et al*. 1983; Pallavicini *et al*. 1983; Fisher *et al*. 1985) and condensation (Antiochos & Sturrock 1982). According to this model, flare loops are created by chromospheric

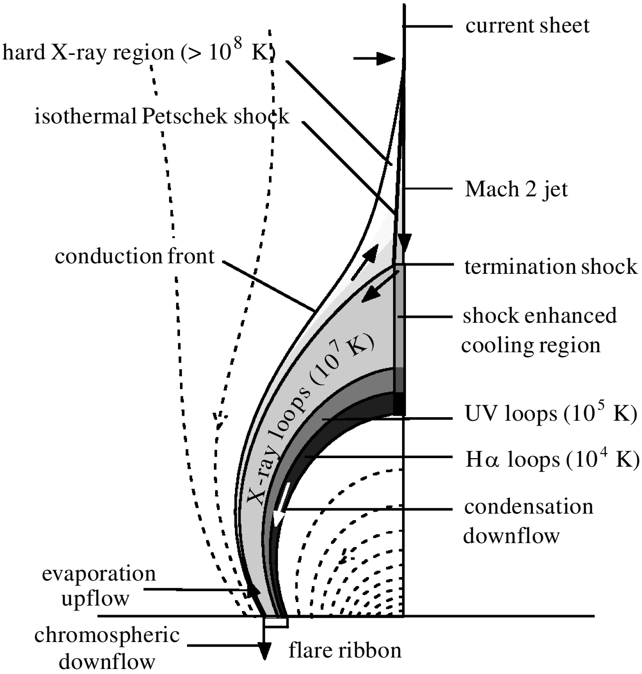

Figure 3. Schematic of a flare loop system formed by reconnection in the supermagnetosonic regime. This regime is most likely to occur in the early phase of a flare when the reconnecting fields are strong. Solid curves indicate boundaries between various plasma regions, while dashed ones indicate magnetic-field lines.

evaporation on field lines mapping to slow-mode shocks in the vicinity of the neutral line (Forbes & Malherbe 1986). These slow shocks are similar to those proposed originally by Petschek (1964), except that the conduction of heat along the field lines causes them to dissociate into isothermal shocks and conduction fronts, as shown in figure 3. The shocks annihilate the magnetic field in the plasma flowing through them, and the thermal energy which is thus liberated is conducted along the field to the chromosphere. This in turn drives an upward flow of dense heated plasma back towards the shocks and compresses the lower regions of the chromosphere downward.

In order for strong slow shocks to form on the field lines below the neutral line, the outflow from it must be supermagnetosonic with respect to the fast-mode wave speed. If the magnetic fields are sufficiently strong, the outflow from the neutral line produces two supermagnetosonic jets, one directed upward and the other downward. Because of the obstacle presented by the closed field lines attached to the photosphere, the lower jet terminates at a fast-mode shock after travelling a short distance (Forbes 1986). Below the termination shock the flow is deflected along the field, and only weak field-aligned slow-mode shocks are present. Consequently, the magnetic energy released below the termination shock is relatively small.

When the magnetic field is relatively strong, the fast-mode Mach number of the jets is about two, but, as the field decreases, the Mach number decreases and the jets eventually become submagnetosonic (Forbes 1986). The transition occurs when the plasma β in the X-ray loops exceeds approximately $(3-\gamma)/\gamma$, where γ is the

PHILOSOPHICAL TRANSACTIONS OF THE ROYAL SOCIETY A MATHEMATICAL, PHYSICAL & ENGINEERING SCIENCES

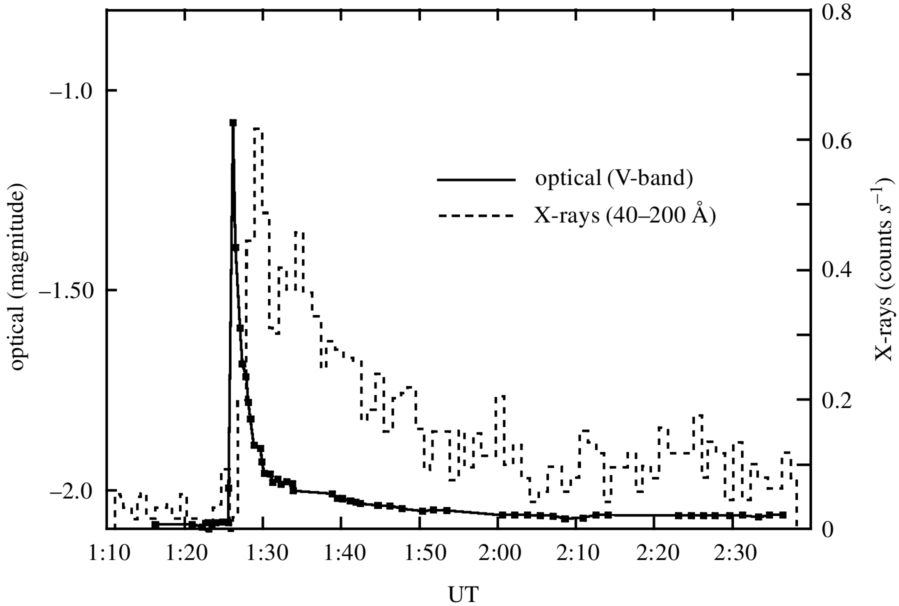

Figure 4. Optical and X-ray light curves for a flare on the red dwarf UV Ceti (23 December 1995). The optical curve is for emissions in the V-band (after de Jager *et al.* 1989).

ratio of specific heats. For $\gamma = \frac{5}{3}$ this gives $\beta = \frac{4}{5}$, which for typical loop parameters corresponds to a field strength of a few gauss (Soward & Priest 1982).

5. Stellar flares

The analysis of stellar flares relies heavily upon the assumption that they are basically similar to solar flares except that they are more energetic (see, for example, Gershberg 1983; Poletto *et al.* 1988). Flare stars can release 10^4 to 10^6 times the amount of energy released by a large solar flare, but it requires only modest increases in magnetic field strengths and scale sizes to account for this extra amount.

Many different types of stars produce flares (see Pettersen (1989) for a review), but the classical flare stars are red dwarfs. These stars constitute *ca.* 65% of the total number of stars in our galaxy, and of these *ca.* 75% are flare stars (Rodonò 1986), including our nearest stellar neighbour, Proxima Centauri. These flare stars are also known as UV Ceti stars (the classic prototype) and dMe or dKe stars. As their name implies, red dwarfs are small stars, having masses of 0.08–0.8$M_\odot$ and radii of 0.15–0.85$R_\odot$, which means they are intrinsically faint (Lang 1992).

The optical radiation produced by a dMe red dwarf during a flare is especially noticeable in the blue continuum, where the contrast with the star's red photospheric light is greatest. There are also Balmer-line enhancements which precede the rise in the blue continuum, but once the continuum appears it dominates the emission lines (Haisch 1989). The emission lines remain enhanced after the continuum fades. As figure 4 shows, the time profile of the continuum is very impulsive, which suggests that the continuum radiation is the stellar counterpart of white-light emission in solar flares. Although solar flares rarely emit any white light at all, when they do, the white light appears only during the impulsive phase in small patches at the photosphere

(Neidig 1989). Similarly, the blue continuum in dMe flares is also associated with the impulsive phase and originates at the star's surface (Van den Oord *et al*. 1996).

Since the mid 1970s, soft X-rays have been detected in numerous flare stars (Haisch 1996). These X-ray emissions occur in the star's corona after the impulsive burst of the optical radiation and are cotemporal with long-lived emission lines such as Hα. The X-rays are thermal in origin and often exhibit the same temporal profile as soft X-rays in solar flares, as shown in figure 4.

Red dwarfs that produce flares are typically fast rotators with deep convection zones. Periods as short as 10 h (compared with 26 days for the Sun) are not unusual, and stars of less than $0.2M_{\odot}$ are thought to be convective throughout (Haisch & Schmitt 1996). The fast rotation, combined with the deep convection zone, greatly enhances dynamo activity in these stars, although the nature of magnetic-field generation in fully convective stars is still an open question.

Flares also occur in early pre-main-sequence stars known as T-Tauri stars. These stars have solar-like masses but are only 10^5 to 10^7 years old. Many are also rapid rotators (Montmerle & Casanova 1996), but the features which make T-Tauri stars especially intriguing are their accretion discs and outflow jets. The jets emanate from the star's polar regions and are fed by the mass inflow from the accretion disc (Gahm 1994).

Close binaries form another important class of flare star. They include the RS Canum Venaticorum (RS CVn) systems, Algol-type binaries and W Ursa Majoris (W Uma) systems, all of which have components that are separated by no more than a few stellar radii. The orbital period of these systems ranges from 0.5 to 50 days (Catalano 1996), and, because the components are tidally locked, the rotation periods of both stars are the same as the orbital period. Thus, as in the case of the dMe stars, close binaries are rapid rotators with strong magnetic dynamos. RS CVn systems consist typically of K and G subgiants located on the main sequence, while the Algol-type binaries consists of a primary star of A or B type with an evolved K subgiant secondary that has overflowed its Roche lobe and is in the process of transferring mass to the primary. The W Uma systems are very short-period (less than one day) contact binaries where both components fill their Roche lobes.

Table 1 compares observed quantities for coronal emission (primarily X-rays) from solar and stellar flares. Two separate solar classes are listed, one for compact flares and one for large flares of long duration. The latter are often referred to as long-duration events, and they are the large-scale two-ribbon flares which produce CMEs. In table 1, Lu is the peak luminosity, W_{r} is the total radiative energy from the flare, integrated over its lifetime, τ_{rise} and τ_{decay} are the rise and decay times of the luminosity curve, $T_{\max}$ is the maximum temperature, E_{m} is the volumetric emission measure, R_* is the stellar radius, h is the height of the flare loops (for solar flares only) and n_{d} is the plasma density deduced from the ratio of density diagnostic lines. (The value of n_{d} for dMe stars is highly uncertain, but is given for completeness.)

The flare luminosity (Lu) is directly proportional to E_{m} times a function which depends only on the temperature (T). Thus, if two flares have the same temperature, but different luminosities, the difference is due to the emission measure (E_{m}).

For the most part, the stellar flares in table 1 are considerably more energetic than their solar counterparts, although there is an overlap between the smallest dMe flares and the largest solar flares. The flares occurring in T-Tauri stars and RS CVn binaries are the largest, with radiative energy outputs that are four to five orders of

Table 1. *Observed quantities for stellar and solar flares in MKS units*

(The densities (n_d) are based on density-sensitive line-ratios. The RS CVn values are from Byrne (1995), while the dMe value is from Schrijver *et al*. (1995). Solar flare values are from Cook *et al*. (1995). Dashes indicate no available data. 1 J = 10^7 erg.)

	red dwarfs (dMe stars)	T-Tauri stars	binaries (RS CVn)	solar: compact	solar: eruptive
Lu (W)	10^{21-23}	10^{23-26}	10^{23-24}	10^{18-20}	10^{20-21}
W_r (J)	10^{24-26}	10^{27-30}	10^{26-29}	10^{22-24}	10^{24-25}
τ_{rise} (s)	10^2	10^{3-4}	10^{2-3}	10^2	10^{2-3}
τ_{decay} (s)	10^{2-3}	10^{4-5}	10^{3-4}	10^3	10^{4-5}
T_{max} (K)	$10^{7.3-7.5}$	$10^{7.3-7.7}$	$10^{7.7-8}$	$10^{7-7.5}$	$10^{7-7.5}$
E_m (m^{-3})	10^{56-59}	10^{58-63}	10^{59-60}	10^{53-55}	10^{55-56}
R_* (m)	$10^{8.3}$	$10^{9.3}$	$10^{8.7}$	$10^{8.8}$	$10^{8.8}$
h (m)	—	—	—	10^{6-7}	10^8
n_d (m^{-3})	10^{17-18}	—	$10^{16.5-18}$	$10^{17-18.5}$	$10^{16.5-17}$

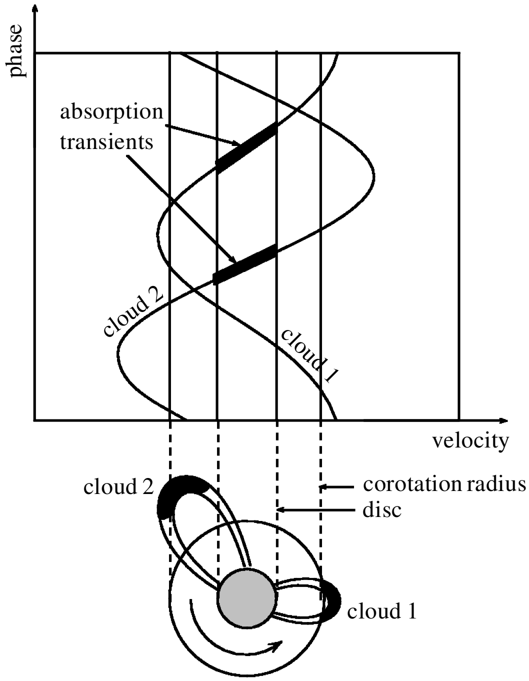

Figure 5. Schematic for AB Doradus showing the relationship between the drift rate of a prominence and its distance from the surface (from Cameron 1996).

magnitude greater than the largest solar flares. Since the densities and temperatures of the stellar flares are comparable to solar flares, the larger energy output of the stellar flares must be due to the involvement of larger volumes.

Recent studies have also revealed the existence of unusually large prominences on some rapidly rotating flare stars (Cameron 1996; Byrne *et al*. 1996). Figure 5 shows the geometry of these prominences inferred from Hα observations of the K-dwarf

AB Doradus. The prominences lie between three and nine stellar radii from the rotation axis, beyond the star's corotation radius at 2.6 stellar radii. Tension in the magnetic loops connecting from the prominences to the stellar surface counterbalances the centrifugal pull of the star's rotation and prevents the prominences from escaping. In contrast to the Sun, the magnetic field helps to hold the prominences down against the rotation rather than holding them up against gravity. The prominences last for several stellar rotations and the amount of mass contained in them approaches 10^{15} kg—a hundred times greater than the mass in a solar prominence. Jeffries (1993) has noted that the stress exerted by the rotating prominences on the field may be the predominant mechanism for storing magnetic energy in the star's corona. If so, the mechanism for triggering flares on AB Doradus may be closely related to the mechanism which generates auroral substorms in Jupiter's magnetosphere. Like AB Doradus, the Jovian magnetosphere is dominated by a rapidly rotating field, and it is the rotational stressing of this field which is thought to supply the magnetic energy for auroral substorms (Zimbardo 1993).

6. Conclusions

There is a general consensus among researchers that both solar and stellar flares are caused by the sudden release of magnetic energy stored in a star's atmosphere. However, the specific mechanisms which cause energy to be stored and then released may be very different. Even for solar flares alone, it is not yet clear whether there is just one mechanism involved or several. It is also quite likely that physical processes such as magnetic reconnection and chromospheric evaporation occur in both solar and stellar flares, but again, the way in which they operate may be very different.

The various mechanisms which have been proposed for flares can be divided into two categories, namely ideal and non-ideal. In the ideal category are those processes, like the MHD kink instability or loss of MHD equilibrium, which do not involve dissipation or diffusion of the magnetic field. In the non-ideal category are those processes which do. The advantage of ideal processes is that they occur on a timescale which is fast enough to account for the rate of energy release at the onset of a flare. However, they must at some stage lead to non-ideal processes in order for the plasma to be heated. This heating can be accomplished by the formation of shocks and current sheets produced by the large-scale motions triggered by the ideal process.

In the near future, new observations of solar flares are likely to reveal much about how magnetic reconnection operates in the solar corona. Although the Japanese satellite Yohkoh has detected X-ray emissions from the site of reconnection in the corona, it remains for future satellite missions to determine if the reconnection process works as any of the existing theories predict.

This work was supported by NASA grants NAGW-4856 and NAG5-1479 to the University of New Hampshire and NAS 8-37334 to the Lockheed-Martin Corporation.

References

Acton, L. W., Feldman, U., Bruner, M. D., Doschek, G. A., Hirayama, T., Hudson, H. S., Lemen, J. R., Ogawara, Y., Strong, K. T. & Tsuneta, S. 1992 The Yohkoh mission for high-energy solar physics. *Science* **258**, 618–625.

Aly, J. J. 1984 On some properties of force-free magnetic fields in infinite regions of space. *Astrophys. J.* **283**, 349–362.

Aly, J. J. 1991 How much energy can be stored in a three-dimensional force-free field? *Astrophys. J.* **375**, L61–L64.

Aly, J. J. 1994 Asymptotic formation of a current sheet in an indefinitely sheared force-free field: an analytical example. *Astron. Astrophys.* **288**, 1012–1020.

Amari, T., Lucianai, J. F., Aly, J. J. & Tagger, M. 1996 Plasmoid formation in a single sheared arcade and application to coronal mass ejections. *Astron. Astrophys.* **306**, 913–923.

Antiochos, S. K. & Sturrock, P. A. 1982 The cooling and condensation of flare coronal plasma. *Astrophys. J.* **254**, 343–348.

Barnes, C. W. & Sturrock, P. A. 1972 Force-free magnetic-field structures and their role in solar activity. *Astrophys. J.* **174**, 659–670.

Bentley, R. D., Doschek, G. A., Simnett, G. M., Rilee, M. L., Mariska, J. T., Culhane, J. L., Kosugi, T. & Watanabe, T. 1994 The correlation of solar flare hard X-ray bursts with doppler blue-shifted soft X-ray flare emission. *Astrophys. J.* **421**, L55–L58.

Byrne, P. B. 1995 Flare in late-type stars: UV. In *Flares and flashes. Proc. IAU Colloq. 151* (ed. J. Greiner, H. W. Duerbeck & R. E. Gershberg), pp. 137–145. Springer.

Byrne, P. B., Eibe, M. T. & Rolleston, W. R. J. 1996 Cool prominences in the corona of the rapidly rotating dMe star, HK Aquarii. *Astron. Astrophys.* **311**, 651–660.

Cameron, A. C. 1996 Stellar prominences. In *Stellar surface structure, IAU Symp. 176* (ed. K. B. Strassmeier & J. L. Linsky), pp. 449–460. Paris: IAU.

Cargill, P. J. & Priest, E. R. 1982 Slow shock heating and the Kopp–Pneuman model for post-flare loops. *Solar Phys.* **76**, 357–375.

Carmichael, H. 1964 A process for flares. In *AAS–NASA Symp. on the Physics of Solar Flares* (ed. W. N. Hess), pp. 451–456, SP-50. NASA.

Catalano, S. 1996 Flares on active binary systems. In *Magnetodynamic phenomena in the solar atmosphere: prototypes of stellar magnetic activity. IAU Colloq. 153* (ed. Y. Uchida, T. Kosugi & H. S. Hudson), pp. 227–234. Dordrecht: Kluwer.

Cheng, C.-C. 1983 Numerical simulations of loops heated to solar flare temperatures. I. Gas dynamics. *Astrophys. J.* **265**, 1090–1102.

Cook, J. W., Keenan, F. P., Dufton, P., Kingston, A. E., Pradhan, A. K., Zhang, H. L., Doyle, J. G. & Hayes, M. A. 1995 The OIV and SIV intercombination lines in solar and stellar ultraviolet spectra. *Astrophys. J.* **444**, 936–942.

Cox, D. P. 1972 Theoretical structure and spectrum of a shock wave in the interstellar medium: the Cygnus loop. *Astrophys. J.* **178**, 143–157.

de Jager, C., Heise, J. & van Genderen, A. M. 1989 Coordinated observations of a large impulsive flare on UV Ceti. *Astron. Astrophys.* **211**, 157–172.

Doschek, G. A., Cheng, C. C., Oran, E. S., Boris, J. P. & Mariska, J. T. 1983 Numerical simulations of loops heated to solar flare temperatures. II. X-ray and UV spectroscopy. *Astrophys. J.* **265**, 1103–1119.

Doschek, G. A., Strong, K. T. & Tsuneta, S. 1995 The bright knots at the tops of soft X-ray loops: quantitative results from Yohkoh. *Astrophys. J.* **440**, 370–385.

Fisher, G. H., Canfield, R. C. & McClymont, A. N. 1985 Flare loop radiative hydrodynamics. V. Response to thick-target heating. VI. Chromospheric evaporation due to heating by nonthermal electrons. VII. Dynamics of the thick-target heated chromosphere. *Astrophys. J.* **289**, 414–441.

Forbes, T. G. 1986 Fast-shock formation in line-tied magnetic reconnection models of solar flares. *Astrophys. J.* **305**, 553–563.

Forbes, T. G. & Malherbe, J. M. 1986 A shock-condensation mechanism for loop prominences. *Astrophys. J.* **302**, L67–L70.

Forbes, T. G. & Malherbe, J. M. 1991 A numerical simulation of magnetic reconnection and radiative cooling in line-tied current sheets. *Solar Phys.* **135**, 361–391.

Forbes, T. G. & Priest, E. R. 1995 Photospheric magnetic field evolution and eruptive flares. *Astrophys. J.* **446**, 377–389.

Furth, H. P., Killeen, J. & Rosenbluth, M. N. 1963 Finite-resistivity instabilities of a sheet pinch. *Phys. Fluids* **6**, 459–484.

Gahm, G. F. 1994 Flares in T Tauri stars. In *Flares and flashes. IAU Colloq. 151* (ed. J. Greiner, H. W. Duerbeck & R. E. Gershberg), pp. 203–211. Springer.

Gershberg, R. E. 1983 On activities of UV Ceti-type flare stars and of T Tauri-type stars. In *Activity in Red-Dwarf Stars. Proc. 71st Colloq. Catania, Italy 1982* (ed. P. B. Byrne & M. Rodonò), pp. 487–495. Dordrecht: Reidel.

Haisch, B. M. 1989 An overview of solar and stellar flare research. *Solar Phys.* **121**, 3–18.

Haisch, B. M. 1996 Stellar X-ray flares. In *Magnetodynamic phenomena in the solar atmosphere: prototypes of stellar magnetic activity. IAU Colloq. 153* (ed. Y. Uchida, T. Kosugi & H. S. Hudson), pp. 235–242. Dordrecht: Kluwer.

Haisch, B. M. & Schmitt, J. J. M. M. 1996 Advances in solar–stellar astrophysics. *Pub. Astron. Soc. Pacific* **720**, 113–129.

Heyvaerts, J. & Priest, E. R. 1976 Thermal evolution of current sheets and the flash phase of solar flares. *Solar Phys.* **47**, 223–231.

Hirayama, T. 1974 Theoretical model of flares and prominences. I. Evaporating flare model. *Solar Phys.* **34**, 323–338.

Hones Jr, E. W., 1973 Plasma flow in the plasma sheet and its relation to substorms. *Radio Sci.* **8**, 979–990.

Hood, A. W. 1990 Structure and stability of solar and stellar coronae. *Computer Phys. Rep.* **12**, 177–203.

Inhester, B., Birn, J. & Hesse, M. 1992 The evolution of line-tied coronal arcades including a convergent footpoint motion. *Solar Phys.* **138**, 257–281.

Jeffries, R. D. 1993 Prominence activity on the rapidly rotating field star HD 197890. *Mon. Not. R. Astron. Soc* **262**, 369–376.

Kopp, R. A. & Pneuman, G. W. 1976 Magnetic reconnection in the corona and the loop prominence phenomenon. *Solar Phys.* **50**, 85–98.

Kusano, K., Suzuki, Y. & Nishikawa, K. 1995 A solar flare triggering mechanism based on the Woltjer–Taylor minimum energy principle. *Astrophys. J.* **441**, 942–951.

Lang, K. R. 1992 *Astrophysical data: planets and stars*. Springer.

Low, B. C. & Smith, D. F. 1993 The free energies of partially open coronal magnetic fields. *Astrophys. J.* **410**, 412–425.

McTiernan, J. M., Kane, S. R., Loran, J. M., Lemen, J. R., Acton, L. W., Hara, H., Tsuneta, S. & Kosugi, T. 1993 Temperature and density structure of the 1991 November 2 flare observed by the Yohkoh soft X-ray telescope and hard X-ray telescope. *Astrophys. J.* **416**, L91–L93.

Martens, P. C. H. & Kuin, N. P. M. 1989 A circuit model for filament eruptions and two-ribbon flares. *Solar Phys.* **122**, 263–302.

Martinell, J. J. 1990 Expansion and stability of a magnetic arcade during a solar flare. *Astrophys. J.* **365**, 342–353.

Masuda, S. 1994 Vertical structure of hard X-ray sources in solar flares. In *New look at the Sun with emphasis on advanced observations of coronal dynamics and flares. Proc. Kofu Symp.* (ed. S. Enome & T. Hirayama), pp. 209–212. Nagano: Nobeyama Radio Observatory.

Mikić, Z. & Linker, J. A. 1994 Disruption of coronal magnetic field arcades. *Astrophys. J.* **430**, 898–912.

Mikić, Z., Barnes, D. C. & Schnack, D. D. 1988 Dynamical evolution of a solar coronal magnetic field arcade. *Astrophys. J.* **328**, 830–847.

Montmerle, T. & Casanova, S. 1996 X-ray flares and variability of young stellar objects. In *Magnetodynamic phenomena in the solar atmosphere: prototypes of stellar magnetic activity. IAU Colloq. 153* (ed. Y. Uchida, T. Kosugi & H. S. Hudson), pp. 247–258. Dordrecht: Kluwer.

Nagai, F. 1980 A model of hot loops associated with solar flares. I. Gasdynamics in the loops. *Solar Phys.* **68**, 351–379.
Neidig, D. F. 1989 The importance of solar white-light flares. *Solar Phys.* **121**, 261–269.
Pallavicini, R., Peres, G., Serio, S., Vaiana, G., Acton, L., Leibacher, J. & Rosner, R. 1983 Closed coronal structures. V. Gasdynamic models of flaring loops and comparison with SMM observations. *Astrophys. J.* **270**, 27–287.
Parker, E. N. 1953 Instability of thermal fields. *Astrophys. J.* **117**, 431–436.
Petschek, H. E. 1964 Magnetic field annihilation. In *The physics of solar flares* (ed. W. N. Hess), pp. 425–439, SP-50. NASA.
Pettersen, B. R. 1989 A review of stellar flares and their characteristics. *Solar Phys.* **121**, 299–312.
Poletto, G., Pallavicini, R. & Kopp, R. A. 1988 Modeling of long-duration two-ribbon flares on M dwarf stars. *Astron. Astrophys.* **201**, 93–99.
Poston, T. & Stewart, I. 1978 *Catastrophe theory and its applications*. San Francisco, CA: Pitman.
Priest, E. R. & Forbes, T. G. 1999 *Magnetic reconnection: MHD theory and application*. Cambridge University Press.
Rodonò M. 1986 The atmospheres of M dwarfs: observations. In *The M-type stars, nonthermal phenomena in stellar atmospheres* (ed. J. R. Johnson & F. R. Querci), pp. 409–453, SP-492. NASA.
Rust, D. M. & Bar, V. 1973 Magnetic fields, loop prominences and the great flares of August, 1972. *Solar Phys.* **33**, 445–459.
Sakao, T., Kosugi, T., Masuda, S., Inda, M., Makishima, K., Canfield, R. C., Hudson, H. S., Metcalf, T. R., Wüsler, J.-P. & Acton, L. W. 1992 Hard X-ray imaging observations by Yohkoh of the 1991 November 15 solar flare. *Publ. Astron. Soc. Japan* **44**, L83–L87.
Schmieder, B., Forbes, T. G., Malherbe, J. M. & Machado, M. E. 1987 Evidence for gentle chromospheric evaporation during the gradual phase of large solar flares. *Astrophys. J.* **317**, 956–963.
Schmieder, B., Heinzel, P., van Driel-Gesztelyi, L., Wiik, J. E. & Lemen, J. 1996 Hot and cool post-flare loops: formation and dynamics. In *Magnetodynamic phenomena in the solar atmosphere: prototypes of stellar magnetic activity. IAU Colloq. 153* (ed. Y. Uchida, T. Kosugi & H. S. Hudson), pp. 211–212. Dordrecht: Kluwer.
Schrijver, C. J., Mewe, R., Van den Oord, G. H. J. & Kaastra, J. S. 1995 EUV spectroscopy of cool stars. II. Coronal structure of selected cool stars observed with the EUVE. *Astron. Astrophys.* **302**, 438–456.
Somov, B. V. 1992 *Physical processes in solar flares*. Dodrecht: Kluwer.
Somov, B. V., Sermulina, B. J. & Spektor, A. R. 1982 Hydrodynamic response of the solar chromosphere to elementary flare burst. II. Thermal model. *Solar Phys.* **81**, 281–292.
Soward, A. M. & Priest, E. R. 1982 Fast magnetic field-line reconnection in a compressible fluid. I. Coplanar field lines. *J. Plasma Phys.* **28**, 335–367.
Steinolfson, R. S. 1991 Coronal evolution due to shear motion. *Astrophys. J.* **382**, 677–687.
Sturrock, P. A. 1968 A model of solar flares. In *Structure and development of solar active regions. IAU Symp. 35* (ed. K. Kiepenheuer), pp. 471–479. Paris: IAU.
Sturrock, P. A. 1991 Maximum energy of semi-infinite magnetic field configurations. *Astrophys. J.* **380**, 655–659.
Sturrock, P. A., Kaufman, P., Moore, R. L. & Smith, D. F. 1984 Energy release in solar flares. *Solar Phys.* **94**, 341–357.
Tsuneta, S. 1993 Solar flares as an ongoing magnetic reconnection process. In *The magnetic and velocity fields of solar active regions. IAU Colloq. 141* (ed. H. Zirin, G. Ai & H. Wang), pp. 239–248. San Francisco, CA: Astronomical Society of the Pacific.

PHILOSOPHICAL TRANSACTIONS OF THE ROYAL SOCIETY A MATHEMATICAL, PHYSICAL & ENGINEERING SCIENCES

Tsuneta, S. 1996 Structure and dynamics of magnetic reconnection in a solar flare. *Astrophys. J.* **456**, 840–849.

Tsuneta, S., Hara, H., Shimizu, T., Acton, L. W., Strong, K. T., Hudson, H. S. & Ogawara, Y. 1992 Observation of a solar flare at the limb with the Yohkoh soft X-ray telescope. *Publ. Astron. Soc. Japan* **44**, L63–L69.

van Ballegooijen, A. A. & Martens, P. C. H. 1989 Formation and eruption of solar prominences. *Astrophys. J.* **343**, 971–984.

Van den Oord, G. H. J., Doyle, J. G., Rodono, M., Linsky, J. L., Haisch, B. M., Pagano, I. & Leto, G. 1996 Flare energetics: analysis of a large flare on YZ Canis Minoris observed simultaneously in the ultraviolet, optical and radio. *Astron. Astrophys.* **310**, 908–922.

Van Tend, W. & Kuperus, M. 1978 The development of coronal electric current systems in active regions and their relation to filaments and flares. *Solar Phys.* **59**, 115–127.

Wolfson, R. & Low, B. C. 1992 Energy buildup in sheared force-free magnetic fields. *Astrophys. J.* **391**, 353–358.

Yeh, T. 1983 Diamagnetic force on a flux tube. *Astrophys. J.* **264**, 630–634.

Zimbardo, G. 1993 Observable implications of tearing-mode instability in Jupiter's nightside magnetosphere. *Planet. Space Sci.* **41**, 357–361.

Discussion

R. Rosner (*The University of Chicago, USA*). In your model of long-enduring events, which is two dimensional, all the energy release is due to reconnection. When you discussed the realistic case, you appealed to three dimensions, and to an ideal MHD instability which drove reconnection (and fixed the short time-scale). In this latter case, which process dominates the release of free energy: the ideal instability or reconnection?

T. G. Forbes. Actually, the driving mechanism in the two-dimensional model is an ideal-MHD loss of equilibrium and not reconnection, and in this two-dimensional model only *ca.* 5% of the stored magnetic energy is released by the ideal process, while 95% is released by the reconnection process which follows it. Although there is no quantitative three-dimensional model as of yet, I would expect the percentage values to be similar.

Y. Uchida (*University of Tokyo, Japan*). We have found that there exist connections from the top of the candle flame type arcade back to the photosphere on both sides. These, together with some other features, cannot be explained by a 'bipolar' model of flares. Together with the energy problem you mentioned as the Aly–Sturrock paradox, we are proposing a 'quadrupole source model', in which the neutral sheet pre-exists in the pre-event configuration, and can avoid the energy difficulty.

T. G. Forbes. It should not be assumed because I showed a model for a dipole configuration that the basic idea of the model will not work if the configuration is other than dipolar. In fact, Eric Priest and I have shown that the model actually works better (in the sense that it releases more energy) if the dipole is replaced by a quadrupole. It is only because the dipole is simpler to discuss that I have concentrated on it.

R. E. Pudritz (*McCaster University, Canada*). T-Tauri stars are known to exhibit strong, flare-like X-ray activity whose origin is still unclear. Have you any thoughts on the applicability of solar flare models to T-Tauri stars?

T. G. Forbes. The T-Tauri systems are so complex that I hesitate even to speculate about the nature of flows in these systems. However, it does seem safe to argue that the volumes involved are probably larger by several orders of magnitude than those for the Sun or red dwarfs. This could be a sign that magnetic interactions between the star and its accretion disc are occurring.

L. Harra (*Mullard Space Science Laboratory, University College London, UK*). You mentioned the cusp-shaped structures in solar flares as an indication of reconnection/eruptive behaviour. In many cases, the cusp structure connects to a small active region/bright point. Does this change the interpretation in any way?

T. G. Forbes. I don't think the basic interpretation that reconnection occurs will change, but the details of what the flow and thermal structures look like should change. It is also good to keep in mind that the models are two dimensional and highly symmetric in order to simplify the mathematics and not because we think this is the way flares are on the Sun. Perhaps when you see field lines radiating out of the top of a cusp curving back down toward the surface, only a small region of a long open arcade actually does this and not the whole arcade.

N. O. Weiss (*University of St Andrews, UK*). Thank you very much. I think that's a word of warning: we should bear in mind that on the one hand there are remarkable similarities between the Sun and the range of middle-aged stars like it (with extensions to much more active stars and to binary stars), but, on the other hand, there might also be fundamental differences.

E. R. Priest (*University of St Andrews, UK*). I would like to thank all our speakers today for demonstrating in no uncertain terms just how vibrant solar research is at the present time, how many fundamental discoveries are being made and how significant they are for other stars and indeed for astrophysics as a whole.

MATHEMATICAL, PHYSICAL & ENGINEERING SCIENCES
THE ROYAL SOCIETY A
PHILOSOPHICAL TRANSACTIONS OF